

OpenECAD: An Efficient Visual Language Model for Computer-Aided Design

Zhe Yuan¹, Jianqi Shi^{1,2}

¹*East China Normal University, Shanghai, China*

²*National Trusted Embedded Software Engineering Technology Research Center, Shanghai, China*

Abstract—Computer-aided design (CAD) tools are utilized in the manufacturing industry for modeling everything from cups to spacecraft. These programs are complex to use and typically require years of training and experience to master. Structured and well-constrained 2D sketches and 3D constructions are crucial components of CAD modeling. A well-executed CAD model can be seamlessly integrated into the manufacturing process, thereby enhancing production efficiency. Deep generative models of 3D shapes and 3D object reconstruction models have garnered significant research interest. However, most of these models are represented in discrete forms. Moreover, the few models based on CAD operations often have substantial input restrictions. In this work, we fine-tuned pre-trained models to create OpenECAD (0.55B, 0.89B, and 4.2B), leveraging the visual, logical, coding, and general capabilities of visual language models. OpenECAD can process images of 3D designs as input and generate highly structured 2D sketches and 3D construction commands. These outputs can be directly used with existing CAD tools' APIs to generate project files. To train our network, we created a new CAD dataset. This dataset is based on existing public CAD datasets, with adjustments and augmentations to meet the requirements of VLM training.

Index Terms—small language model, visual language model, computer aided design, automated CAD design, 2D-3D shape modeling, geometric deep learning, machine learning

I. INTRODUCTION

Using 3D shape representation aligns with human intuition. In today's digital era, computer-aided design (CAD) tools are employed in various industrial fields for 3D shape design, including automotive, aerospace, manufacturing, and architectural design. However, due to drafting conventions and the requirements for shape constraints and edit-ability, 3D shapes are still based on 2D sketches. This approach allows for the meticulous development, relation, and annotation of all design details, mirroring the precision of traditional draftsmen.

A typical 3D part drawing process involves multiple "Sketch-Extrusion" steps. The relationship between sketch and extrusion is not strictly one-to-one; a single sketch can correspond to multiple extrusions, and one extrusion can be composed of multiple sketches. A sketch consists of multiple closed loops formed by several lines and includes constraints within or between them to ensure the sketch is fully defined. The extrusion operation generates a 3D feature based on the 2D sketch(s). Generally, there is a sequential relationship between "Sketch-Extrusion" steps, as a sketch's reference plane may rely on an existing face in the model, and constraints within the Sketch may depend on points or lines already

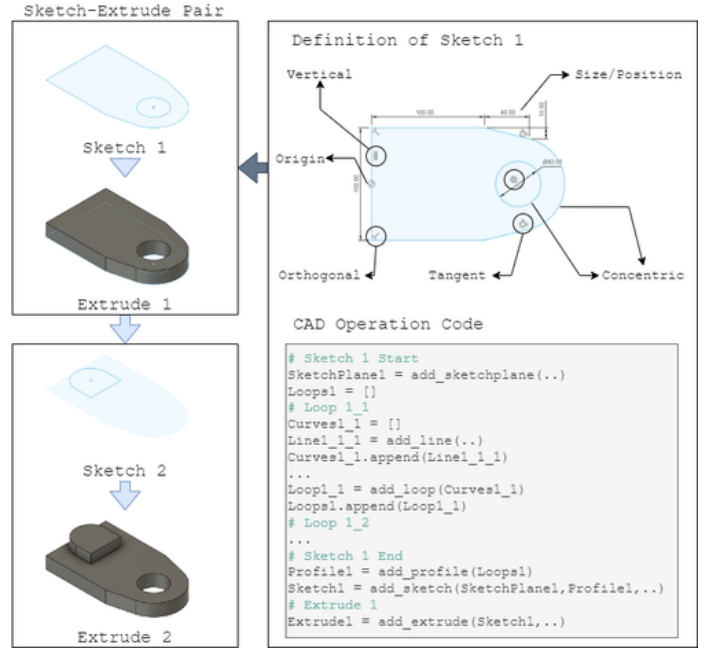


Fig. 1. A schematic diagram of the process for drawing 3D parts using CAD tools.

present in the model. As shown in Figure 1, this is a simple process for drawing 3D parts.

There has been extensive research on 3D model generation. However, most of this research focuses on creating computer-discretized forms of 3D shapes, such as 3D point clouds [1]–[5], voxelized shapes [6]–[9], polygon meshes [10]–[12], and levelset fields [13]–[17]. This approach neglects the essence of 3D shape design—the drawing process. In practical applications, the generated models often do not fully meet the requirements, and other steps in the production process may necessitate design modifications. Consequently, modifications to the generated models are frequently needed. However, due to the absence of the drawing process, modifying these models can be less efficient than manually modeling from scratch, making these methods challenging to apply in real-world scenarios.

To address this issue, some studies have emerged with the development of neural networks. Since 3D shapes are still based on 2D sketches, these studies can be divided into 2D sketch generation and 3D CAD model generation. Sketch-

Graphs [18] provides a dataset of constrained 2D sketches, CurveGen and TurtleGen [19] generate closed curve sketches, and CADL [20] uses language models to generate sketches. For 3D model generation, SolidGen [21] and ComplexGen [22] generate B-rep models, while Point2Cyl [23], DeepCAD [24], and Free2CAD [25] generate CAD command sequences. It is worth noting that these models often have significant input limitations. For example, they may require existing 3D point clouds, may not accept inputs to limit how to generate, or require isometric hand-drawn sketches. These constraints still differ significantly from existing manual modeling workflows, making it challenging to apply them in production processes.

Now, with the development of language models and multimodal language models, these limitations are expected to be overcome. Multimodal language models can flexibly accept various forms of input and understand their meaning, thereby constraining the output. Currently, multimodal language models already have the capability to accept model images and program code and describe their meaning in simple language. For example, GPT-4o can possess simple 3D shape's generation and has understanding capabilities, and many language models can interpret program code. Therefore, in this work, we leverage the visual, logical, coding, and general capabilities of visual language models to make the following contributions:

- 1) Based on existing public CAD datasets, such as SketchGraphs [18], Fusion 360 Gallery [26], and DeepCAD [24], we convert these datasets into "image-CAD operation code" pairs, including 2D sketch generation and 3D shape generation. Using currently available multimodal large language models, such as GPT-4o, we generate high-quality annotated datasets. Additionally, we utilize rendering tools to generate various forms of images to enhance the versatility of model inputs.
- 2) Based on existing public small language models and multimodal small language models, such as TinyLLaMA [27], OpenELM [28], Phi3 [29], and TinyLLaVA [30], we train them using the aforementioned training sets and test their performance in CAD design.
- 3) Design a program standard for CAD operations that can interface with the APIs of various CAD tools, enabling the generated model code to be directly used in CAD applications.

II. RELATED WORK

A. Small Language and Visual Language Models

Small language models have recently become very popular due to the growing demand for privacy and local execution. Small language models are those that are smaller in size and require fewer computational resources, allowing them to run on local devices and ensure data privacy and security. Despite their smaller size, these models can still deliver efficient performance on specific tasks, making them suitable for resource-constrained environments. Currently available small language models include Microsoft's Phi series [29], Apple's OpenELM [28] and TinyLLaMA [27], based on Meta's LLaMA [31].

Multimodal small language models further expand the applications of small language models. These models can process not only text data but also understand and generate data in various modalities, such as images and audio. By integrating information from multiple modalities, these models excel in a wider range of tasks. For example, they can convert image descriptions into text or transform hand-drawn sketches into structured textual information. Currently available multimodal small language models include the TinyLLaVA series [30], based on small language models above, and Microsoft's Phi3 Vision [29].

B. Generative models of 3D shapes' CAD commands

Currently, there are several models designed for generating CAD commands for 2D Sketches or 3D shapes. SketchGraphs [18] provides a dataset of constrained 2D sketches and proposes corresponding generative models. CurveGen and TurtleGen [19] aim to generate usable sketches by producing closed curves, ignoring non-essential constraint solving. CADL [20] focuses on defining sketch operations as structures similar to programming languages, leveraging language models for sketch generation.

For 3D model generation, approaches can be divided into models generating B-rep and those generating CAD commands, depending on the final output. The Boundary representation (B-rep) format is the de-facto shape representation in CAD for modeling solid and sheet objects. B-rep has poorer editability compared to other formats but can accommodate simple model modifications. SolidGen [21] and ComplexGen [22] can both generate B-rep models. Models generating CAD commands can directly output CAD command sequences. Point2Cyl [23] can convert cylindrical 3D point clouds into CAD command sequences. DeepCAD [24] provides a dataset of CAD command sequences and proposes a model capable of generating sequences randomly. Free2CAD [25] can convert hand-drawn isometric sketches into CAD command sequences.

As these are traditional small models, they have significant input and output limitations, making integration with existing manual modeling workflows challenging. However, they offer high-quality and structurally complete datasets, which provide a foundation for generating training data for multimodal small language models. To our knowledge, there are currently no multimodal small language models specifically trained for generating CAD commands for 3D shapes.

III. METHOD

We now present our OpenECAD dataset and model, which includes a new CAD command sequence format designed for language models (see Figure 2). The dataset has been improved based on existing CAD datasets and utilizes large language models to generate high-quality natural language descriptions of CAD models. We fine-tuned pre-trained vision-language models based on small language models, resulting in the OpenECAD models that are compact in size and capable of running locally, specifically designed for CAD applications.

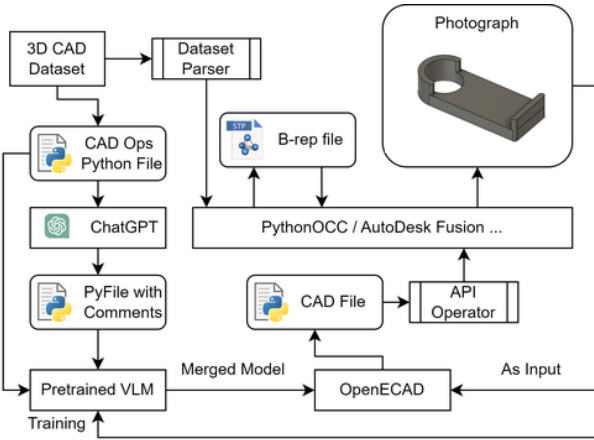


Fig. 2. Overview of the OpenECAD Dataset and Model.

A. Design and Generation of Datasets

CAD models can be represented in various ways. At the user interaction level with CAD software, 3D shapes are described by a series of CAD operations to create solid forms. For instance, to model a simple table, a user begins by sketching on a 2D plane, drawing a rectangle (a closed curve) and constraining its dimensions. After completing the sketch, the user extrudes it to form the tabletop and constrains its thickness. Next, the user sketches on the existing model, drawing four squares (four closed curves) and constraining their dimensions. After completing this sketch, the user extrudes these shapes to form the table legs, merging them with the previous model and constraining their height. This completes the modeling of a simple table (see Figure 3). This process constitutes a CAD operation sequence, consisting of two Sketch-Extrusion pairs. Clearly, this CAD operation sequence can be described in natural language, as demonstrated above. Additionally, the 2D view of a CAD model is the most intuitive way to express it to humans, akin to the flowchart mentioned above.

In this work, we aim to generate CAD operation sequences using visual language models. CAD operation sequences not only interact with CAD software but also have meanings understandable by humans, allowing modifications and applications in other design processes. To constrain the generation of CAD operation sequences, we use human-understandable inputs such as model images or textual descriptions. Therefore, our dataset includes pairs of target model images as input with CAD operation codes and descriptions as output, pairs of target models as input with CAD operation codes as output, and pairs of target model images and descriptions as input with CAD operation codes as output. These datasets encompass both 3D CAD models and pure 2D sketches to enhance the model's ability to generate and constrain 2D sketches.

1) *Definition of the Code Format for CAD Operation Sequences:* Mature CAD tools support a rich set of commands, most of which are simplified calls to collections of basic commands—for example, a rectangle is a collection of four line segments and some constraints. However, in practice, only

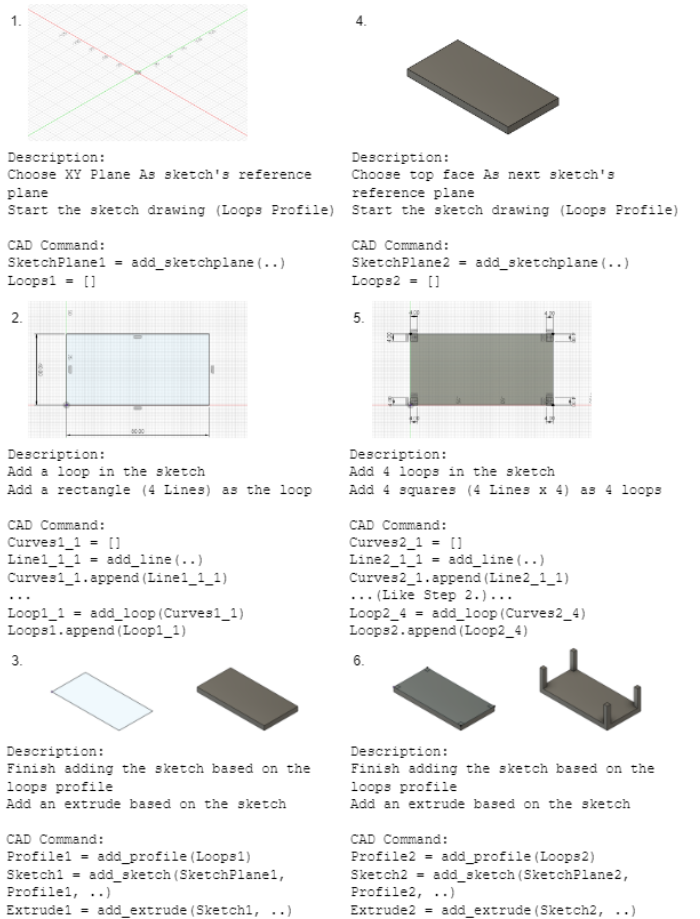


Fig. 3. A CAD Command Sequence Diagram for Drawing a Table.

a small subset of these commands is widely used. Therefore, we currently consider only the most basic and commonly used commands in our dataset (see Table I). Due to the versatility of language models, extending the dataset later is relatively easy.

Sketch. Sketch is the core of CAD operations. Extrusion is built upon Sketch. Curves and constraints form closed loops within a Sketch. Multiple closed loops make up the profile of a closed region. In our representation, the definition of Sketch begins with defining the sketch reference plane, similar to most CAD tools. We then maintain a list of loops and start drawing curves and adding constraints. Once a loop is completed, it is stored in the list. After all loops are completed, the corresponding profile is generated, and finally, the sketch is created based on the reference plane and the profile. The sketch reference plane is defined by the three-dimensional coordinates of the origin and the direction of the sketch's XY axes.

Curves and Constraints. In practice, we consider three types of widely used curve commands: drawing a line, drawing an arc, and drawing a circle. We also consider nine types of widely used constraint commands: making a line horizontal or vertical, fixing the size of a curve, making two points of curves coincident, making two lines parallel, perpendicular, or having

TABLE I
CAD COMMANDS AND THEIR PARAMETERS.

Command Name	Parameters
Curves Series	
add_line	start_point, end_point
add_arc	start_point, end_point, mid_point
add_circle	center_point, radius
Constraints Series	
make_horizontal(vertical)	line0
fix_size	curve0, size
make_coincident	point0, point1
make_parallel	line0, line1
make_perpendicular	line0, line1
make_tangent	curve0, curve1
make_mirror	curve0, curve1 (same type)
make_angle	line0, line1, clockwise
Sketch and its helper	
add_sketchplane	origin_point, x_axis, y_axis
add_profile	loops_list
add_sketch	sketchplane, profile
Extrusion	
add_extrude	sketch, operation, type, extent_size

a fixed angle, and making two curves tangent or mirrored.

Extrusion. The extrusion command extrudes a sketch from a 2D plane into a 3D body. The extrusion type can be one-sided, symmetric, or two-sided with respect to the sketch plane. The command also specifies how to merge the newly extruded 3D body with the previously created shape using one of the operations: creating a new body, or joining, cutting, or intersecting with the existing body.

All operation names are chosen to be as meaningful as possible to aid the language model in understanding and using them. With these operation commands, we describe a CAD model as a sequence of executable commands in code.

2) *Translation of CAD Operation Sequences:* According to the definitions provided in the previous section, we can convert any CAD model covered by the described operations (in Table I) into a CAD operation sequence as defined by us. However, in practice, different CAD tools or datasets may have slight variations in their definitions of CAD operations. We need to ensure the equivalence of CAD operations before and after the conversion. In this section, we will use the three types of curves we defined as examples to illustrate (see Figure 4), from the perspective of curve degrees of freedom (DoFs), how we ensure the equivalence of CAD models or datasets in other formats when converting them to our code.

Line. According to the definition, a line is defined by two points: the start point and the end point. Since each point has 2 DoFs, a line has 4 DoFs. For a line defined by a start point, direction vector, and length, the start point has 2 DoFs, the length has 1 DoF, and although the direction vector has 2 DoFs, its length information is irrelevant for the line, contributing only 1 DoF. Therefore, lines defined by both methods have 4 DoFs and can be equivalently converted between each other using an algorithm.

Arc. According to the definition, an arc is defined by three points: the start point, end point, and midpoint. Since the midpoint must lie on the perpendicular bisector of the line

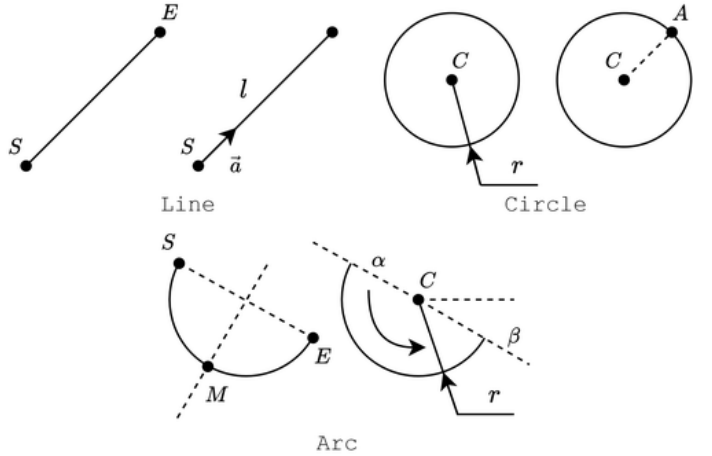


Fig. 4. Comparison Diagram of Two Definitions for Line, Arc, and Circle.

segment defined by the start and end points, an arc has 5 DoFs. For an arc defined by the center, absolute angles of the start and end edges, radius, and clockwise direction, the DoFs are also evidently 5. Therefore, arcs defined by both methods have 5 DoFs and can be equivalently converted between each other using an algorithm.

Circle. According to the definition, a circle is defined by its center and radius, having 3 degrees of freedom (DoFs). For a circle defined by its center and a point on the circle, there are 4 DoFs. If we ignore the orientation of the circle (since in some CAD tools, operations like mirroring and rotating use the circle's orientation), then the point on the circle only serves to define the radius, and its specific position is internal information of the circle. Therefore, it can be reduced to 3 DoFs. Thus, circles defined by both methods have 3 DoFs and can be equivalently converted between each other using an algorithm.

Based on the above principles, we have developed scripts to convert other CAD models or datasets into CAD operation sequence codes for training our VLM.

3) *Generation of Natural Language Descriptions for CAD Models:* Describing CAD models in natural language is crucial for understanding 3D shapes. Adding these descriptions as annotations to the CAD operation sequence code can help people quickly grasp the meaning of each code segment and swiftly locate and modify the necessary parts. To construct natural language descriptions corresponding to CAD operation sequence codes, we employed existing large language models such as GPT-4o. By using prompts and examples, we added natural language annotations to the existing CAD operation sequence codes. The prompt used was: "Please add comments to the drawing code below to indicate what shape is drawn by each section of the code. Don't add comment for every line or arc." To prevent the language model from adding annotations to every CAD operation (like drawing lines or arcs), we constrained the model to add annotations by operation units, such as drawing a rectangle, etc.

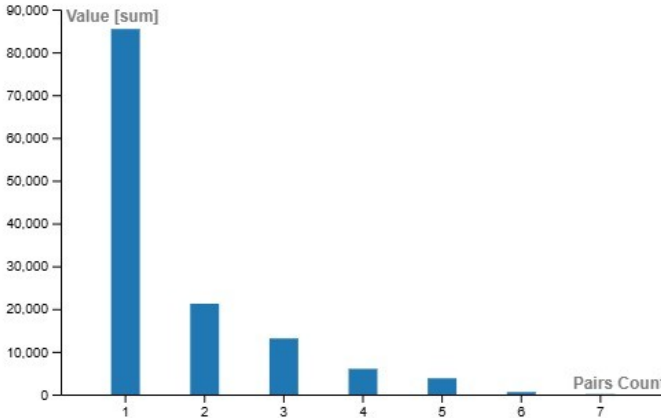


Fig. 5. The statistical distribution of the number of "Sketch-Extrusion" steps in OpenECAD 3D dataset.

4) *Generation of CAD Model View Images*: We have introduced how to define and generate CAD model codes and textual descriptions, providing text materials for VLM training. In this section, we will briefly explain how to generate image materials for VLM training, specifically by creating 2D views of CAD models. We first use the PythonOCC [32] tool to write scripts that generate step files (B-Rep format) based on the CAD operation sequence codes. Then, we render the step files using PythonOCC. Finally, we select a direction that forms a random angle with the isometric view direction vector to generate 2D views as image materials.

5) *Creation of CAD Dataset*: Based on the above method, we generated a 3D CAD dataset derived from the DeepCAD dataset [24] and a 2D CAD dataset derived from the Sketch-Graphs dataset [18]. We excluded designs that were generated incorrectly or had overly long CAD command sequences due to the number of tokens that small language models can accept is limited, resulting in a total of 130,239 3D designs and 628,499 2D sketches. The statistical distribution of the number of "Sketch-Extrusion" steps in the 3D dataset is shown in the Figure 5. The statistical distribution of the number of curves and constraints operations in the 2D dataset is shown in the Figure 6.

B. Training Vision Language Model

1) *The choice of language model foundation and multimodal approach*: Due to the high confidentiality requirements of manufacturing enterprises and the substantial CPU and GPU resources typically occupied by CAD design tools, we chose OpenELM [28] (450M) and Phi-3 mini [29] (3.8B) with relatively small parameter sizes as the foundation for our language model. OpenELM is an efficient language model family developed by Apple. It employs a layer-wise scaling strategy to allocate parameters efficiently within each layer of the transformer model. This approach enhances accuracy while maintaining computational efficiency. Phi-3, developed by Microsoft Research, is another series of advanced small language models (SLMs). This series includes Phi-3-mini

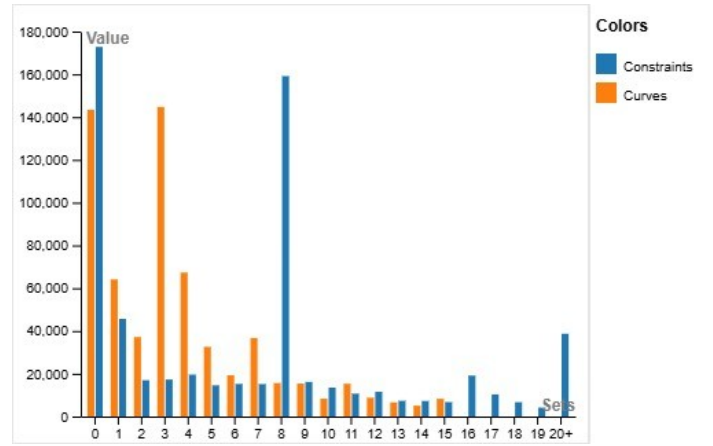


Fig. 6. The statistical distribution of the number of curves and constraints operations in OpenECAD 2D dataset.

(3.8B), Phi-3-small (7B), and Phi-3-medium (14B), each with different parameter sizes. Despite their compact parameter scales, Phi-3 models achieve language understanding and reasoning capabilities comparable to larger models. These models are trained on high-quality data and optimized algorithms. It is worth noting that the context acceptance length for OpenELM (450M) is 2048 tokens. In contrast, Phi-3 has a minimum context acceptance length of 4096 tokens, with an option to use a version supporting up to 128k tokens at the cost of some content accuracy.

To endow the language model foundation with multimodal capabilities, we selected OpenAI's CLIP [33] and Google's [34] as visual encoders for OpenELM (450M). These models are trained on large datasets consisting of images paired with corresponding text descriptions, combining visual and textual information to make predictions.

To train the entire model with multimodal conversational abilities, we employed the LLaVA [35] method and its dataset. LLaVA combines a visual encoder and a large language model in an innovative multimodal approach, enabling comprehensive visual and language understanding. LLaVA uses GPT-4 to generate multimodal language-image instruction data. For training the model, we utilized the training framework provided by TinyLLaVA [30].

For Phi-3 mini, since Microsoft has already released its multimodal version, Phi-3 Vision (4.2B), which was trained using methods similar to LLaVA, we will directly use the pre-trained model provided by Microsoft.

2) *Fine-tuning on a pre-trained visual language model*: To enable the general visual-language model to generate CAD code, we fine-tuned it using the LoRA [36] method on the pre-trained OpenELM-CLIP and OpenELM-SigLIP models. LoRA stands for Low-Rank Adaptation of Large Language Models. In the field of natural language processing (NLP), there is a common paradigm that involves large-scale pre-training on general domain data followed by adaptation to specific tasks or domains. However, as we pre-train larger models, fully fine-tuning all model parameters becomes less feasible

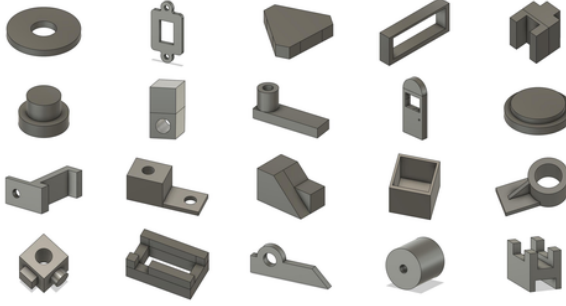


Fig. 7. Example illustrations of CAD designs for evaluating.

TABLE II
SCORING TABLE.

Scoring Item	Score (out of 100)
Is the code executable?	10
Accuracy of 3D shape construction	90
For each Loop-Extrusion pair (out of 100)	
- 2D sketch positioning	20
- Accuracy of 2D Loop	60
- 3D operation	20

due to computational costs. LoRA proposes a novel approach. Instead of full fine-tuning, LoRA freezes the pre-trained model weights and injects trainable rank decomposition matrices into each layer of the Transformer architecture. This significantly reduces the number of trainable parameters for downstream tasks.

We performed LoRA fine-tuning on the pre-trained OpenELM-CLIP (0.55B) and OpenELM-SigLIP (0.89B) models using an Nvidia GeForce GTX 1080 Ti (11 GB VRAM). The Rank and Alpha for LoRA were set to 128 and 256, respectively. Training for one epoch with our 3D dataset took approximately 60 hours. Through fine-tuning, we obtained the OpenECAD 0.55B and 0.89B models.

Similarly, we used an Nvidia GeForce RTX 4090 D (24 GB VRAM) to perform LoRA fine-tuning on the Phi-3 Vision (4.2B) model. The LoRA rank and alpha were set to 256 and 512, respectively. Training with our dataset for one epoch took approximately 20 hours. Through fine-tuning, we obtained OpenECAD 4.2B model.

IV. EXPERIMENTS

A. Evaluation Metrics

For a given 3D shape, there are often multiple methods to create it using CAD tools. Moreover, the input views of the model generally lack dimensional information, meaning the generated model only adheres to the proportional relationships visible in the image. Therefore, directly comparing the generated CAD operation sequence codes is not reasonable. To address this, we designed a scoring algorithm and created several test CAD designs (see Figure 7). We used specific views of these designs as input images for evaluation, serving as a metric for assessing the model's generation capability.

1) Scoring Algorithm for Evaluating Outputs: To assess the generative capability of our model, we designed a scoring algorithm. First, the algorithm verifies if the generated code can be executed directly by the API operator to create a model. If it cannot run, it scores 0 points. If it can run, we then use a visual language model (such as GPT-4o) to compare the generated model's view with the target input, evaluating each basic feature. Each basic feature corresponds to a 2D loop. We separately evaluate the loops in the 2D sketches during the modeling process to ensure precise assessment, as these loops may or may not be considered a single sketch during modeling.

We score the results based on executability and the correctness of the 3D shapes (see Table II). Each Loop-Extrusion pair is considered a basic 3D shape. If the number of generated Loop-Extrusion pairs is insufficient, points will be deducted proportionally. For each Loop-Extrusion pair, we score based on the reference plane position of the 2D sketch, the extrusion operation, and the drawing of the 2D loop. The specific calculation method is shown in the following formula.

$$score = 10R + \frac{90}{N_s} \sum_{i=1}^{N_s} (20P_i + 20O_i + 60L_j) \quad (1)$$

where R denotes executability, N_s represents the number of Loop-Extrusion pairs, P_i and O_i indicate the correctness of the 2D sketch position and 3D extrusion operation for the i -th Sketch-Extrusion pair, and L_j denotes the accuracy of the curves within the loop. $R, P_i, O_i, L_j \in [0, 1]$.

B. CAD Designs for Test

To test the model, we require high-quality CAD designs. We extracted approximately 100 3D designs from the training set, maintaining a ratio of 10:5:3:2 for designs containing 1, 2, 3, and 4 or more Sketch-Extrusion pairs, respectively. After filtering and removing duplicates, we obtained 57 unique 3D designs. These designs were redrawn using CAD tools such as AutoDesl Fusion, and appropriate views were selected to generate the input images. Some examples are shown in the Figure 7. The resolution of the images is 640x400.

C. Evaluation Results

1) The Inference Speed of the Models: The input was standardized to a 640x400 image of a 3D shape, with the prompt:

"This image is a view of a 3D model from a certain angle. Please try to use Python-style APIs to render this model."

For OpenECAD 0.55B and 0.89B, we used an Nvidia GeForce GTX 1080 Ti (11 GB VRAM) for inference, with a peak memory usage of less than 5GB. Getting a 3D shape's code took approximately 20 seconds. For OpenECAD 4.2B, we used an Nvidia GeForce RTX 4090 D (24 GB VRAM) for inference, with a peak memory usage of less than 17GB. Getting a 3D shape's code took approximately 45 seconds.

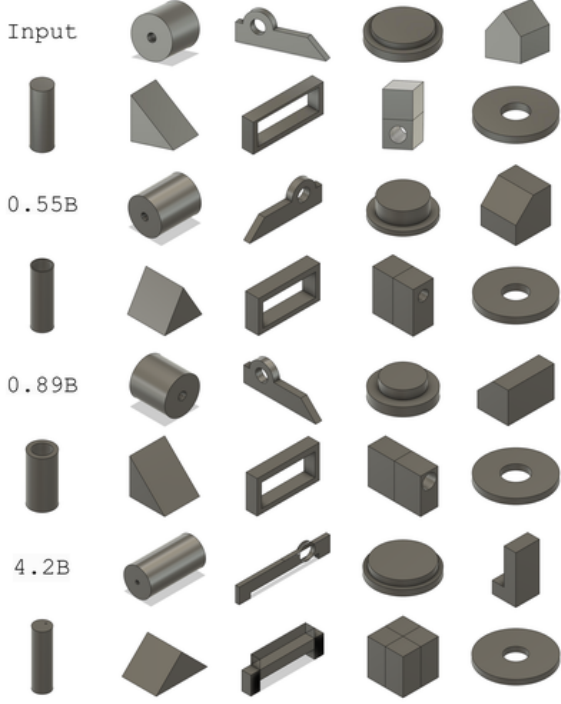


Fig. 8. Comparison of some successful rendered test results illustrations.

2) *Generating Code and Rendering*: We tested OpenECAD versions 0.55B, 0.89B, and 4.2B, and also tested GPT-4o. Since GPT-4o was not trained for the use case described in this paper, we used the following prompt for testing:

"I am going to provide you with a 3D shape's corresponding Python code for its modeling process. After that, I will input images of other 3D shapes, and please provide the corresponding Python code for them. """OpenECAD style Code Example."''' This image is a view of a 3D model from a certain angle. Please write the codes of it in the format above."

During the testing of OpenECAD, the maximum number of new tokens that 0.55B, 0.89B, and 4.2B models can generate is 1536, 1024, and 3092, respectively. Due to these context limitations, there are instances where the generated code is incomplete (see Table III). GPT-4o, due to its support for a longer context, did not encounter issues with incomplete code generation.

Similar to generating datasets, we use the PythonOCC tool to write a library that attempts to directly run the generated code to create CAD projects and output them as STEP files (B-Rep format). Then, we use PythonOCC to render the STEP files to obtain views. Since the generated programs from the model cannot ensure complete accuracy, errors may occur that the API operator cannot handle, leading to model rendering failures (see Table III).

Based on the scoring method mentioned above, we obtained the scores, the number of executable results, the number of incomplete results, the number of runtime errors, and the number of completely correct results for each model, as shown in the Table III.

TABLE III
EVALUATION RESULTS TABLE.

Model	Overall Score	Executable	Unfinished	Run with Errors	Completely Correct
0.55B	30.77	21	21	15	11
0.89B	29.74	17	35	5	16
4.2B	40.63	37	4	16	10
GPT-4o	11.40	38	0	19	0

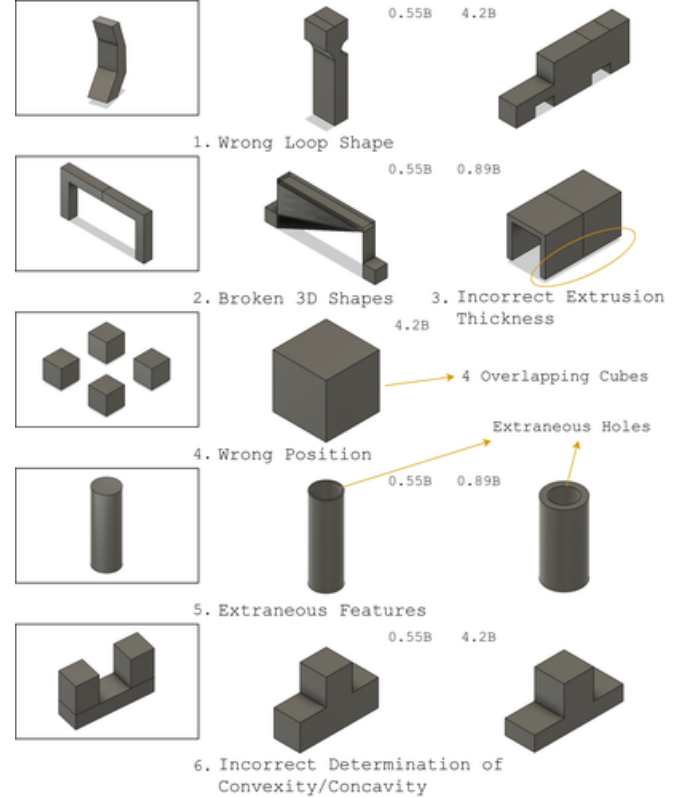


Fig. 9. Typical errors in generated results.

D. Analysis of OpenECAD's outputs

From Table III, it is evident that OpenECAD 0.55B and 0.89B perform similarly. However, the 0.89B model uses more tokens for image input, reducing the number of new tokens it can generate. This leads to a higher number of incomplete outputs compared to the 0.55B model, resulting in a slightly lower overall score. The 4.2B model has the highest relative score but generates fewer fully correct results than the 0.55B and 0.89B models. This could be because its longer context length affects its code generation capability. All OpenECAD models significantly outperform the unfinetuned GPT-4o, whose only advantage is its extremely long context length, allowing it to complete the entire code.

In the generated results, several typical errors were observed (see Figure 9), including:

- Case 1: For complex irregular shapes, the corresponding sketch could not be generated correctly.
- Case 2: Errors in generating the 2D sketch profile, possibly due to intersections between loops leading to

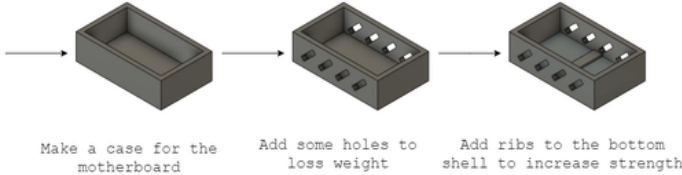


Fig. 10. An example of a real-world application of the model.

damaged extrusions.

- Case 3: Incorrect extrusion size ratios.
- Case 4: Incorrect sketch positioning in subsequent steps when multiple "Sketch-Extrusion" steps are present.
- Case 5: Difficulty in distinguishing between solid and hollow cylinders, as the relevant features are hard to observe in this view.
- Case 6: Difficulty in distinguishing between convex and concave shapes, leading to incorrect model generation.

Based on the above results and typical errors, we can infer the current shortcomings of the OpenECAD model:

- Weak ability to handle complex sketches, unable to reasonably determine the dimensions of various curves.
- Poor capability in generating correctly sized dimensions.
- Limited ability to construct complex models.
- Insufficient detail recognition when interpreting drawings.
- Lack of compact command sequences, leading to overly long contexts.

Based on the above, our future work will focus on expanding the types of CAD operations supported in the dataset, enhancing the model's visual resolution and segmentation capabilities, improving the language model's coding abilities, and increasing the model's ability to control size and proportion.

E. Future Applications

Currently, OpenECAD primarily serves as a simple CAD operation generation model, focusing on generating models from images. However, by improving the dataset, we can train models using similar methods and apply them to downstream applications (like Figure 10). These applications include, but are not limited to:

- Assisting users in operating CAD design tools by guiding them on how to proceed with CAD operations to build or modify models based on their requirements and existing CAD actions.
- Enhancing the ability to handle user CAD needs, such as design reusability and designing connectors for existing parts.
- Introducing CAE-related knowledge to the model to address some CAE issues, such as structural reinforcement, material reduction, and kinematic simulation, during the CAD phase.

V. DISCUSSION AND CONCLUSION

For CAD model generation, our approach has some limitations. Currently, we only consider three of the most widely used curve command types (lines, arcs, and circles), but other curve commands can be easily added. We also only consider using a single image as a reference, with the model attempting to generate the complete output result rather than step-by-step outputs. Not every CAD command sequence code currently generates a topologically valid shape. Our network cannot guarantee the correctness of its output. In practice, with sufficient context length, the number of failed executions of the generated CAD command sequence codes is relatively low.

To address these limitations, more work needs to be done. Enhancements to the dataset should include support for multi-view perspectives, complex curves, and textual requirements. The code generation process should be improved to better integrate with CAD tools, allowing the model to generate code incrementally, similar to how humans draw while referencing the design, rather than outputting the entire CAD code at once.

In summary, we have introduced OpenECAD, a visual language model and its accompanying dataset designed for generating CAD operation sequence codes. OpenECAD aims to address the challenge of CAD model generation using visual language models and has successfully generated some relatively simple 3D shapes.

ACKNOWLEDGMENT

We extend our gratitude to DeepCAD [24] and Sketch-Graphs [18] for their contributions to CAD dataset development, to TinyLLaVA [30] for providing the visual language model training framework, and to Apple [28] and Microsoft [29] for developing language models that empower developers.

REFERENCES

- [1] P. Achlioptas, O. Diamanti, I. Mitliagkas, and L. Guibas, "Learning representations and generative models for 3d point clouds," in *International conference on machine learning*, pp. 40–49, PMLR, 2018.
- [2] Y. Yang, C. Feng, Y. Shen, and D. Tian, "Foldingnet: Point cloud auto-encoder via deep grid deformation," in *Proceedings of the IEEE conference on computer vision and pattern recognition*, pp. 206–215, 2018.
- [3] K. Mo, P. Guerrero, L. Yi, H. Su, P. Wonka, N. Mitra, and L. J. Guibas, "Structurenet: Hierarchical graph networks for 3d shape generation," *arXiv preprint arXiv:1908.00575*, 2019.
- [4] G. Yang, X. Huang, Z. Hao, M.-Y. Liu, S. Belongie, and B. Hariharan, "Pointflow: 3d point cloud generation with continuous normalizing flows," in *Proceedings of the IEEE/CVF international conference on computer vision*, pp. 4541–4550, 2019.
- [5] R. Cai, G. Yang, H. Averbuch-Elor, Z. Hao, S. Belongie, N. Snavely, and B. Hariharan, "Learning gradient fields for shape generation," in *Computer Vision–ECCV 2020: 16th European Conference, Glasgow, UK, August 23–28, 2020, Proceedings, Part III 16*, pp. 364–381, Springer, 2020.
- [6] R. Girdhar, D. F. Fouhey, M. Rodriguez, and A. Gupta, "Learning a predictable and generative vector representation for objects," in *Computer Vision–ECCV 2016: 14th European Conference, Amsterdam, The Netherlands, October 11–14, 2016, Proceedings, Part VI 14*, pp. 484–499, Springer, 2016.
- [7] J. Wu, C. Zhang, T. Xue, B. Freeman, and J. Tenenbaum, "Learning a probabilistic latent space of object shapes via 3d generative-adversarial modeling," *Advances in neural information processing systems*, vol. 29, 2016.

[8] J. Li, K. Xu, S. Chaudhuri, E. Yumer, H. Zhang, and L. Guibas, “Grass: Generative recursive autoencoders for shape structures,” *ACM Transactions on Graphics (TOG)*, vol. 36, no. 4, pp. 1–14, 2017.

[9] Y. Liao, S. Donne, and A. Geiger, “Deep marching cubes: Learning explicit surface representations,” in *Proceedings of the IEEE Conference on Computer Vision and Pattern Recognition*, pp. 2916–2925, 2018.

[10] T. Groueix, M. Fisher, V. G. Kim, B. C. Russell, and M. Aubry, “A papier-mâché approach to learning 3d surface generation,” in *Proceedings of the IEEE conference on computer vision and pattern recognition*, pp. 216–224, 2018.

[11] N. Wang, Y. Zhang, Z. Li, Y. Fu, W. Liu, and Y.-G. Jiang, “Pixel2mesh: Generating 3d mesh models from single rgb images,” in *Proceedings of the European conference on computer vision (ECCV)*, pp. 52–67, 2018.

[12] C. Nash, Y. Ganin, S. A. Eslami, and P. Battaglia, “Polygen: An autoregressive generative model of 3d meshes,” in *International conference on machine learning*, pp. 7220–7229, PMLR, 2020.

[13] Z. Chen and H. Zhang, “Learning implicit fields for generative shape modeling,” in *Proceedings of the IEEE/CVF conference on computer vision and pattern recognition*, pp. 5939–5948, 2019.

[14] L. Mescheder, M. Oechsle, M. Niemeyer, S. Nowozin, and A. Geiger, “Occupancy networks: Learning 3d reconstruction in function space,” in *Proceedings of the IEEE/CVF conference on computer vision and pattern recognition*, pp. 4460–4470, 2019.

[15] J. J. Park, P. Florence, J. Straub, R. Newcombe, and S. Lovegrove, “Deepsdf: Learning continuous signed distance functions for shape representation,” in *Proceedings of the IEEE/CVF conference on computer vision and pattern recognition*, pp. 165–174, 2019.

[16] Z. Chen, A. Tagliasacchi, and H. Zhang, “Bsp-net: Generating compact meshes via binary space partitioning,” in *Proceedings of the IEEE/CVF conference on computer vision and pattern recognition*, pp. 45–54, 2020.

[17] R. Wu, Y. Zhuang, K. Xu, H. Zhang, and B. Chen, “Pq-net: A generative part seq2seq network for 3d shapes,” in *Proceedings of the IEEE/CVF Conference on Computer Vision and Pattern Recognition*, pp. 829–838, 2020.

[18] A. Seff, Y. Ovadia, W. Zhou, and R. P. Adams, “Sketchgraphs: A large-scale dataset for modeling relational geometry in computer-aided design,” *arXiv preprint arXiv:2007.08506*, 2020.

[19] K. D. Willis, P. K. Jayaraman, J. G. Lambourne, H. Chu, and Y. Pu, “Engineering sketch generation for computer-aided design,” in *Proceedings of the IEEE/CVF conference on computer vision and pattern recognition*, pp. 2105–2114, 2021.

[20] Y. Ganin, S. Bartunov, Y. Li, E. Keller, and S. Saliceti, “Computer-aided design as language,” *Advances in Neural Information Processing Systems*, vol. 34, pp. 5885–5897, 2021.

[21] P. K. Jayaraman, J. G. Lambourne, N. Desai, K. D. Willis, A. Sanghi, and N. J. Morris, “Solidgen: An autoregressive model for direct b-rep synthesis,” *arXiv preprint arXiv:2203.13944*, 2022.

[22] H. Guo, S. Liu, H. Pan, Y. Liu, X. Tong, and B. Guo, “Complexgen: Cad reconstruction by b-rep chain complex generation,” *ACM Transactions on Graphics (TOG)*, vol. 41, no. 4, pp. 1–18, 2022.

[23] M. A. Uy, Y.-Y. Chang, M. Sung, P. Goel, J. G. Lambourne, T. Birdal, and L. J. Guibas, “Point2cyl: Reverse engineering 3d objects from point clouds to extrusion cylinders,” in *Proceedings of the IEEE/CVF Conference on Computer Vision and Pattern Recognition*, pp. 11850–11860, 2022.

[24] R. Wu, C. Xiao, and C. Zheng, “Deepcad: A deep generative network for computer-aided design models,” in *Proceedings of the IEEE/CVF International Conference on Computer Vision*, pp. 6772–6782, 2021.

[25] C. Li, H. Pan, A. Bousseau, and N. J. Mitra, “Free2cad: Parsing freehand drawings into cad commands,” *ACM Transactions on Graphics (TOG)*, vol. 41, no. 4, pp. 1–16, 2022.

[26] K. D. D. Willis, Y. Pu, J. Luo, H. Chu, T. Du, J. G. Lambourne, A. Solar-Lezama, and W. Matusik, “Fusion 360 gallery: A dataset and environment for programmatic cad construction from human design sequences,” *ACM Transactions on Graphics (TOG)*, vol. 40, no. 4, 2021.

[27] P. Zhang, G. Zeng, T. Wang, and W. Lu, “Tinyllama: An open-source small language model,” 2024.

[28] S. Mehta, M. H. Sekhavat, Q. Cao, M. Horton, Y. Jin, C. Sun, I. Mirzadeh, M. Najibi, D. Belenko, P. Zatloukal, and M. Rastegari, “OpenELM: An Efficient Language Model Family with Open Training and Inference Framework,” *arXiv.org*, Apr. 2024.

[29] M. Abdin, S. A. Jacobs, A. A. Awan, J. Aneja, A. Awadallah, H. Awadalla, N. Bach, A. Bahree, A. Bakhtiari, H. Behl, *et al.*, “Phi-3 technical report: A highly capable language model locally on your phone,” *arXiv preprint arXiv:2404.14219*, 2024.

[30] B. Zhou, Y. Hu, X. Weng, J. Jia, J. Luo, X. Liu, J. Wu, and L. Huang, “Tinyllama: A framework of small-scale large multimodal models,” 2024.

[31] H. Touvron, T. Lavril, G. Izacard, X. Martinet, M.-A. Lachaux, T. Lacroix, B. Rozière, N. Goyal, E. Hambro, F. Azhar, A. Rodriguez, A. Joulin, E. Grave, and G. Lample, “Llama: Open and efficient foundation language models,” 2023.

[32] T. Paviot, “pythonocc,” Dec. 2022.

[33] A. Radford, J. W. Kim, C. Hallacy, A. Ramesh, G. Goh, S. Agarwal, G. Sastry, A. Askell, P. Mishkin, J. Clark, *et al.*, “Learning transferable visual models from natural language supervision,” in *International conference on machine learning*, pp. 8748–8763, PMLR, 2021.

[34] X. Zhai, B. Mustafa, A. Kolesnikov, and L. Beyer, “Sigmoid loss for language image pre-training,” in *Proceedings of the IEEE/CVF International Conference on Computer Vision*, pp. 11975–11986, 2023.

[35] H. Liu, C. Li, Q. Wu, and Y. J. Lee, “Visual instruction tuning,” *Advances in neural information processing systems*, vol. 36, 2024.

[36] E. J. Hu, Y. Shen, P. Wallis, Z. Allen-Zhu, Y. Li, S. Wang, L. Wang, and W. Chen, “Lora: Low-rank adaptation of large language models,” *arXiv preprint arXiv:2106.09685*, 2021.